



UNIVERSITY OF LEEDS

This is a repository copy of *Assessment of beam-column connections using perforated beams with multiple closely spaced web openings*.

White Rose Research Online URL for this paper:
<http://eprints.whiterose.ac.uk/87513/>

Version: Accepted Version

Proceedings Paper:

Tsavdaridis, KD and Papadopoulos, T (2015) Assessment of beam-column connections using perforated beams with multiple closely spaced web openings. In: 8th International Conference on Behaviour of Steel Structural in Seismic Areas. The 8th STESSA Conference on Behaviour of Steel Structural in Seismic Areas, 01-03 Jul 2015, Shanghai, China. .

Reuse

Unless indicated otherwise, fulltext items are protected by copyright with all rights reserved. The copyright exception in section 29 of the Copyright, Designs and Patents Act 1988 allows the making of a single copy solely for the purpose of non-commercial research or private study within the limits of fair dealing. The publisher or other rights-holder may allow further reproduction and re-use of this version - refer to the White Rose Research Online record for this item. Where records identify the publisher as the copyright holder, users can verify any specific terms of use on the publisher's website.

Takedown

If you consider content in White Rose Research Online to be in breach of UK law, please notify us by emailing eprints@whiterose.ac.uk including the URL of the record and the reason for the withdrawal request.



eprints@whiterose.ac.uk
<https://eprints.whiterose.ac.uk/>

ASSESSMENT OF BEAM-COLUMN CONNECTIONS USING PERFORATED BEAMS WITH MULTIPLE CLOSELY SPACED WEB OPENINGS

Konstantinos Daniel Tsavdaridis* and Theodore Papadopoulos**

* Assistant Professor of Structural Engineering, School of Civil Engineering, University of Leeds, LS2 9JT, Leeds, UK
e-mail: k.tsavdaridis@leeds.ac.uk

** Design Engineer, Pell Frischmann Consultants, 5 Manchester Square, W1U 3PD, London, UK
e-mail: TPapadopoulos@pellfrischman.com

Keywords: RWS connections, perforated beams, web openings, cellular, seismic design, cyclic loading

Abstract. Recently researchers concentrate on alternative fuse designs promoting the concept of performance-based design while reducing the beam section in different ways including that of creating a hole in its web (RWS connections). Similar practice is applied in the fabrication of perforated beams mostly used to support the service integration as well as the significant mass reduction in steel frames. This paper presents a finite element (FE) analysis of a partially restrained extended end-plate connection with single and multiple circular web perforations introduced along the length of the beam and subjected to the cyclic loading proposed by SAC protocol from FEMA-350 (2000). The parameters introduced were the distance from the face of the column, S , and the number of closely spaced web openings. The design of such connections should be based on the *articulate decision of the first opening's distance from the face of the column*.

1 INTRODUCTION

Steel moment resisting frames (MRFs) have traditionally been built in areas susceptible to high seismicity and are greatly dependent on their beam-to-column connection behaviours. In the past, fully welded connections were considered to provide the optimum combination of strength, stiffness and ductility which according to codes are the major factors in the seismic design of joints [1, 2].

A more recent trend of earthquake resistant design comes by the name of performance-based design. Reduced Beam Section (RBS) or “Dogbone” connections with different ways of reducing locally the cross-sectional area of the beams are embracing this concept by achieving material efficiency. Popov et al. in 1998 studied the pre-Northridge connections, analysed their brittle failure and proposed two remedy designs using either a Dogbone or reinforcing plates [3]. Works by Lee and Kim in 2007 and Pachoumis et al. in 2009 also exhibited satisfactory levels of connection ductility with the plastic hinge forming at the reduced section area without fracture being developed [4, 5]. Recently, a pioneer concept of merging the purposely weakened beams/connections with the use of perforated beams was introduced, as a trend of achieving material efficiency and considering material reduction through beam web cuts, also known as Reduced Web Section (RWS) [6]. Perforated beams offer the advantages of a deeper web (i.e. increased second moment of area) depending on the manufacturing procedure, but without the increase in weight; hence reduced material volume without a decrease of the bending capacity. They can therefore span longer distances as well as incorporate services within the floor-to-ceiling structural zone, as it is shown in Figure 1. There has been a lot of research on perforated beam webs with the geometry of the perforation ranging from circular, hexagonal, to even elliptically-based shapes [7, 8, 9]. However, very limited research has been conducted up to date regarding the design limitations of connections when such standard and non-standard perforated beams are used.



Figure 1. Circular shaped Reduced Web Sections incorporating services (SteelConstruction.info, Image courtesy of ASD Westok Ltd.).

2 REDUCED WEB SECTIONS (RWS) CONNECTIONS

Research undertaken in RWS connections is related to the fabrication process (increased cost due to web cutting and welding of the section), buckling issues (i.e. stability issues due to the increased depth in certain cases), number of web perforations as well as their use in MRFs.

RWS connections provide a higher rotational capacity of the order of 0.05radian, whilst 0.035radian is suggested by EC8 and FEMA-350 to be acceptable in seismic design [2, 10]. On the other hand, the local shear capacity of the beams is decreased because of the opening existence. Nowadays' trend is to increase the rotational capacity of connections from what was suggested by post-Northridge codes.

Recent research was conducted for the seismic-resistant design of MRFs using beams with isolated web openings by Yang et al. in 2009 [11]. Both experimental and numerical analyses performed were subjected to pseudo-dynamic, quasi-static and push-over actions. Strong emphasis was put in analysing the failure modes while avoiding brittle fracture. The comparison with typical un-perforated (solid webbed) beam-to-column connections as well as with connections consisting one of the three different typical sizes of circular web openings was established. All results revealed a ductile failure of the frame with adequate stiffness which was not restricted significantly by the presence of the web openings. The focus on the beam-to-column connections promoted the creation of the Vierendeel mechanism with no brittle web fracture. It is worth to note that the Vierendeel mechanism is a ductile failure mode with the formation of four plastic hinges and the redistribution of the load in the vicinity of the opening [13].

3 PARAMETRIC STUDIES

3.1 Introduction

A semi-rigid steel beam-to-column connection with circular beam web openings is examined while subjected to cyclic loading. Only conventional circular web openings are used, while the web-post buckling behaviour is extensively analysed by having multiple closely spaced web openings along the length of the beam. The structural performance of the RWS connection with the use of perforated beams, instead of one local perforation (i.e. local weakening) at the cross-sectional area of the beam and with the connection being partially restrained, has not yet been examined under cyclic loading.

In order to fully understand the response of RWS connections with perforated beams and evaluate their ability to dissipate seismic energy, numerous FE models including a solid beam model with no perforations is developed. A total of 12 FE models were developed and categorised into four Sets. The same connection configuration from Díaz et al. (2011) (specimen T101.010) is used in this study, whilst the length from the end-plate to the load application point, L_{load} , is different [12]. The beam length was increased in order to be able to accommodate periodical multiple web openings and simulate a typical span of 6m. Consequently, L_{load} was extended from 1.25m in the literature to 3m in the parametric Sets.

3.2 Parameters

The parameters examined generally can be seen in Figure 2 and are as follows:

- The number of web opening
- The shape of web openings ranging from standard to non-standard web openings
- The web opening depth, d_o
- The distance from the face of the column to the centreline of the web opening, S
- The distance between adjacent web openings taken from their respective centreline, S_o

It is worth to note that in some models the beam's flanges have been restrained in the transverse direction to the web and/or include column stiffeners in order to avoid the pre-mature lateral torsional buckling (LTB) of the deep webbed and slender perforated beams as well as the high stresses concentration in the shear panel zone.

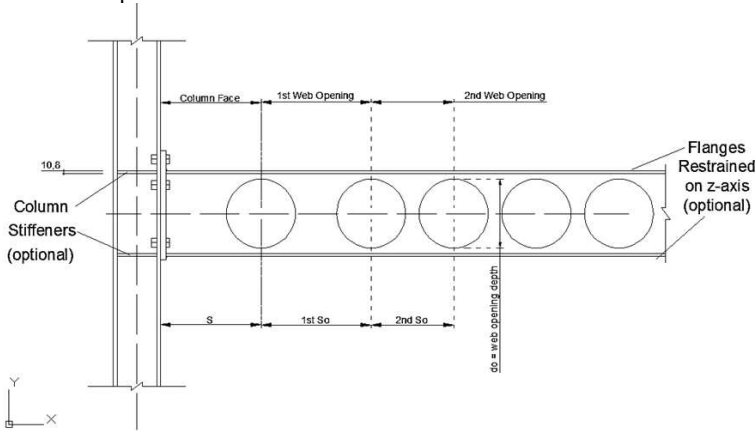


Figure 2. Semi-rigid beam-to-column connection showing geometrical parameters.

For all analyses, the web opening depth, d_o , is taken as equal to $0.8h_b$, where h_b is the height of the beam.

$$d_o = 0.8 \times h_b = 0.8 \times 0.2989 = 0.239 \text{ m} \quad (1)$$

Three values of the distance, S , are examined (200mm, 350mm and 520mm). Tsavdaridis et al. in 2014 suggested that the parameter S proved to be dependent on the opening's geometry [6]. The value of 200mm was taken to account for the worst case scenario of having a large WOA and a small distance S which would maximise the stress concentrations near the face of the column. Better performance by moving the stresses away from the face of the column is anticipated by increasing the distance S up to a certain point that would still mobilise the stresses. Tsavdaridis and D'Mello in 2011 also investigated the effect of eight S_o/d_o ratios ranging from 1.1 to 1.8 [7]. For closely spaced web openings the optimum ratios were found to be from 1.1 to 1.3, while adequate web-post behaviour was found when novel elliptically-based web openings were utilised. The distance between adjacent circular web openings, S_o , for closely spaced openings is therefore taken as equal to $1.2d_o$, while for largely spaced openings, $S_o=1.6d_o$.

$$S_o = 1.2 \times d_o = 1.2 \times 0.8 \times h_b = 1.2 \times 0.23912 = 0.286 \text{ m} \quad (\text{closely spaced}) \quad (2)$$

$$S_o = 1.6 \times d_o = 1.6 \times 0.8 \times h_b = 1.6 \times 0.23912 = 0.382 \text{ m} \quad (\text{widely spaced}) \quad (3)$$

3.3 Loading Sequence and Analysis

The specimen was loaded cyclically according to the SAC loading protocol recommended by FEMA-350. Beam end displacements are applied at the location of the beam's vertical stiffener, with an upward

and a downward displacement producing one cycle of the loading protocol. A total of 32 cycles, equivalent to 64 applied displacements, are computed. Table 1 summarises the displacements values, ΔLC , applied as load steps. Distance LLC from the centreline of the column to the centreline of the load stiffener is equal to:

$$LLC = L_{load} + t_{ep} + h_c/2 = 3 + 0.02 + 0.1625/2 = 3.10125 \text{ m} \quad (4)$$

Table 1. Beam end displacements for cyclic loading sequence.

| Number of Cycles | Peak Deformation ϕ (radians) | Load Steps (Accumulative) | End Displacements ΔLC (m) |
|------------------|--------------------------------------|------------------------------|--------------------------------------|
| 6 | 0.00375 | 12 | 0.0116297 |
| 6 | 0.005 | 24 | 0.0155063 |
| 6 | 0.0075 | 36 | 0.0232594 |
| 4 | 0.01 | 44 | 0.0310125 |
| 2 | 0.015 | 48 | 0.0465188 |
| 2 | 0.02 | 52 | 0.0620250 |
| 2 | 0.03 | 56 | 0.0930375 |
| 2 | 0.04 | 60 | 0.1240500 |
| 2 | 0.05 | 64 | 0.1550625 |

An Eigen buckling analysis is initially produced to derive the first Eigen mode shape, introducing small imperfections, which then used as the basis to update the model's geometry after being scaled by a recommended factor of $t_w/200=7.3/200=0.0365\text{mm}$. A nonlinear (geometric and material) analysis is then performed with the full 64 load steps using the "Newton-Raphson" approach.

3.4 Parametric FE Results and Discussion

All twelve models are organised into four Sets, with the hysteretic behaviour and stress distribution being scrutinised in all cases to the ease of comparison and with scope to establish meaningful results despite the large number of geometric parameters assessed. In this paper two Sets with seven models, including the solid beam connection model, are presented and discussed.

3.4.1 Parametric Set 1 (Solid Model and Models 1, 2 and 3)

Table 2. Parametric Set 1.

| Model | Number of Holes | Column Face Distance, S | Web Opening Spacing, S_o | Second Web Opening Distance | Material Properties |
|-------|------------------|----------------------------|-------------------------------|-----------------------------------|-----------------------|
| Solid | --- | --- | --- | --- | As experimental study |
| 1 | 1 hole | 200 | --- | --- | As experimental study |
| 2 | 2 holes | 200 | 1.2 | 1.2 | As experimental study |
| 3 | Fully perforated | 200 | 1.2 | 1.2 | As experimental study |

| Model | Column Stiffeners | Flanges Restrained |
|-------|-------------------|--------------------|
| Solid | --- | --- |
| 1 | --- | --- |
| 2 | --- | --- |
| 3 | --- | --- |

Moment-rotation curves, referred to as hysteretic curves in the case of cyclic loading with multiple loading-unloading loops, are used to obtain information about the beam-to-column connection including the initial rotational stiffness, rotational capacity, strength (ultimate moment capacity) as well as the amount of energy dissipated. The hysteretic curves are established from information derived by ANSYS

Multiphysics v.14 FE software; vertical y-axis nodal displacements are recorded at the column centreline and at the end of the beam where the stiffener is located, and reactions corresponding to the applied displacement for each load step. The four hysteretic curves are superposed and shown in Figure 3.

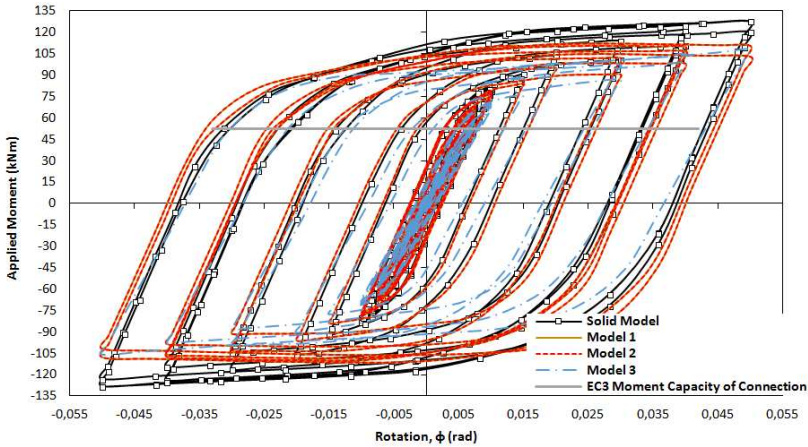


Figure 3. Moment-rotation curves of solid beam model and Models 1, 2 and 3.

Comparing the four hysteretic behaviours, as it was anticipated the solid beam model without perforations achieves the highest moment capacity of approximately 125kNm. Therefore, there is a decrease in moment capacity for the case of Model 1 and Model 2 (110 and 115kNm, respectively), whereas the lowest moment capacity is achieved by the fully perforated beam (Model 3 with 10 openings) with 105kNm. However, it is worth mentioning that perforated beams are usually deeper than the initial parent solid sections, hence the moment capacity in such cases should not be reduced significantly and the design is counterbalance by this principle. Further observations are made regarding the ultimate rotational capacity of each specimen. It is also remarkable that all specimens achieved an ultimate rotational capacity of about 0.05radian making RWS connections suitable in Special or Intermediate Moment Frame (SMF or IMF) systems as well as in seismically active zones applications. It is concluded that the introduction of web openings has reduced the total moment capacity without reducing the ultimate rotational capacity. The fully-perforated Model 3 shows an increased ductility of the connection and lower strength degradation towards the final cycles when compared to the solid beam or Model 1. Generally, all models examined show a relatively gradual strength degradation which is in accordance to Tsavdaridis et al. (2014) observations, as this is typical of beams with deep web openings (0.8h) [6]. Table 3 summarises the results derived from the hysteretic curves. The initial rotational stiffness is calculated from the first cycle of the analysis. The Web Opening Area (WOA) corresponds to the area of the perforation and the energy dissipated, E , is equivalent to the area under the hysteretic curve which is computed using the trapezoidal rule.

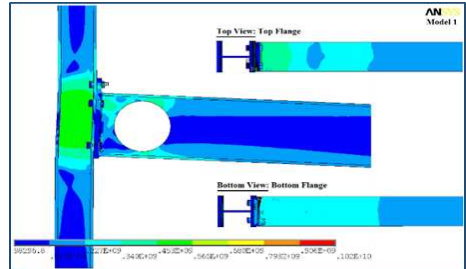
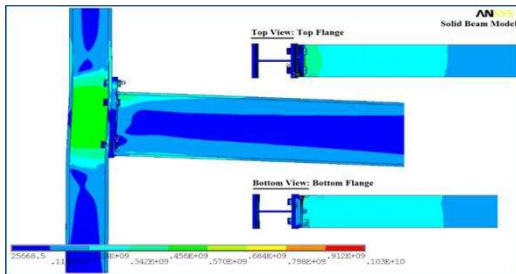
Table 3. Results Summary Table.

| Model | Number of Holes | Yield Moment M_y (kNm) | Ultimate Moment M_u (kNm) | Yield Rotation ϕ_y (rad) | Ultimate Rotation ϕ_u (rad) |
|-------|------------------|--------------------------|-----------------------------|-------------------------------|----------------------------------|
| Solid | N/A | 74.59 | 128.58 | 0.009592 | 0.049989 |
| 1 | 1 hole | 71.14 | 112.19 | 0.009492 | 0.050025 |
| 2 | 2 holes | 64.41 | 117.23 | 0.009292 | 0.050025 |
| 3 | Fully perforated | 62.44 | 105.77 | 0.008555 | 0.050004 |

| Model | Rotational Ductility D_ϕ | Initial Rotational Stiffness K_i (kNm/rad) | Web Opening area (mm ²) | Dissipated Energy E (kNm)(rad) |
|-------|-------------------------------|--|-------------------------------------|--------------------------------|
| Solid | 5.21 | 10329.89 | - | 107.14 |
| 1 | 5.27 | 10240.98 | 44907.8 | 92.5 |
| 2 | 5.38 | 9167.77 | 44907.8 | 81.19 |
| 3 | 5.85 | 8097.76 | 44907.8 | 45.94 |

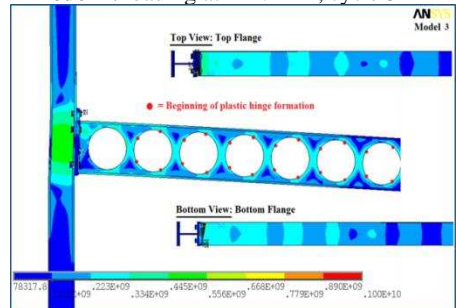
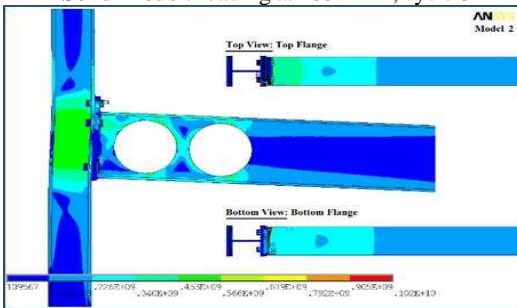
It is observed that the initial rotational stiffness slightly decreases with the introduction of web openings. When the two extreme cases were plotted, the initial rotational stiffness was found higher for the specimen with the solid beam model. The rotational stiffness decreased by 1%, 11.3% and 21.6% for the Model 1, Model 2 and Model 3, respectively. The horizontal threshold line in Figure 3 corresponds to the moment capacity of the connection (52.5kNm) as calculated using EC3.

More analytical, the introduction of multiple web openings (ten holes) reduces the moment capacity by 17.7% while the ultimate rotation was almost unchanged in all cases. Consequently, the dissipated energy is higher for the solid beam case since higher moment capacity, provided that the column and the connection is strong enough to withstand the forces acting from the beam without developing plastic hinges on columns, and hence the soft-storey phenomenon. In order to fully understand the lack of dissipated energy in certain cases, the stress distribution was investigated. The above results demonstrate that all the geometrical parameters introduced can affect the behaviour of the connection in different ways. Therefore, von-Mises stresses for all four models are plotted in Figure 4. As it was aforementioned, in order to mobilise the stresses away from the column and the connection, in the vicinity of beam web perforations, a Vierendeel mechanism should be formed.



Solid Model: loading at 155.1mm, cycle 32

Model 1: loading at 124.1mm, cycle 31



Model 2: loading at 124.1mm, cycle 31

Model 3: loading at 93.1mm, cycle 28

Figure 4. Von-Mises stress contour plots of Set 1.

It is observed that the introduction of perforations has mobilised stresses towards the beam. It is also found that all three models reduced the amount of stress in the panel zone, without though, shifting the stresses entirely to the beam. The full plastic hinges are not formed at this stage as the stress (between 350 and 400MPa) has not reached the ultimate strength of the beam of 445MPa. High stresses found in the column's panel zone and in the top row of bolts, hence the Vierendeel mechanism was not completely formed. Hence, it was concluded that factors such as the connection type, the size of the column in relation to the beam, as well as the material properties play significant role in the formation of the Vierendeel mechanism.

Introducing an additional second perforation (Model 2), more stress is dissipated from the critical region into the second hole. The second hole has mobilised more stresses and a pattern of four plastic hinges begun to appear at various angles, however the stress magnitude in the panel zone of the column is still high in this specific example. Stresses in the top and bottom flanges are moved further away from the column, while the high stress intensity in the top flange, due to the top row of bolts, is slightly decreased. The close distance between the perforations ($1.2d_o$), also results in the high stress concentration in the area of the web-post. Adding more perforations, the high stresses in the shear panel zone decreased gradually (Model 3). Plastic hinges developed with stresses diminishing further away from the beam-to-column connection. The final position of the plastic hinges is the same for all circular openings, except the first one which is located very close to the joint and is subjected to excessive shear forces. The highest stresses along the beam are found in the vicinity of the first two perforations (first web-post to the connection), as discussed in Model 2.

All four models achieved an acceptable ultimate rotational capacity to be used in seismic resistant design. While the introduction of perforations reduced the strength of the beam and consequently reduced the moment capacity of the connection as well as the initial rotational stiffness, the ultimate rotational capacity and the rotational ductility were increased. Large openings in the range of $0.8h$ were proved in previous studies to promote the creation of four plastic hinges and experience little to no local web buckling when located at certain positions.

However, the parameters used in this first Set are not considered as ideal for design. The following changes are proposed: (i) having uniform material strengths of S355 steel and M10 bolts, so as to not hinder the desired weak beam-strong column mechanism to form and (ii) increasing the distance S from the face of the column, so as to investigate the critical location (threshold) of the first opening. Since this study is focusing on the introduction of cellular beams in the design of MRFs, fully perforated beams will be used for the rest of the investigation.

3.4.2 Parametric Set 2 (Models 9, 10 and 11)

Table 4. Parametric Set 2.

| Model | Number of Holes | Column Face Distance, S | Web Opening Spacing, S_o | Second Web Opening Distance | Material Properties |
|-------|------------------|---------------------------|----------------------------|-----------------------------|-------------------------|
| 9 | Fully perforated | 200 | 1.2 | 1.2 | S355 (Class 10.9 Bolts) |
| 10 | Fully perforated | 350 | 1.2 | 1.2 | S355 (Class 10.9 Bolts) |
| 11 | Fully perforated | 520 | 1.2 | 1.2 | S355 (Class 10.9 Bolts) |

| Model | Column Stiffeners | Flanges Restrained |
|-------|-------------------|--------------------|
| 1 | YES | YES |
| 2 | YES | YES |
| 3 | YES | YES |

All specimens in Set 2 are using fully perforated beams. The material properties are uniform and column stiffeners are added to obtain an improved response avoiding the lateral torsional buckling phenomenon observed in certain thin-webbed perforated beams with large and closely spaced web

openings. The flanges have been restrained on the transverse direction (z-axis) to investigate whether this technique influences the web buckling behaviour. Three distances, S , are examined: 200mm, 350mm and 520mm. All hysteretic curves from Set 2 are plotted and superposed for the ease of comparison in Figure 5.

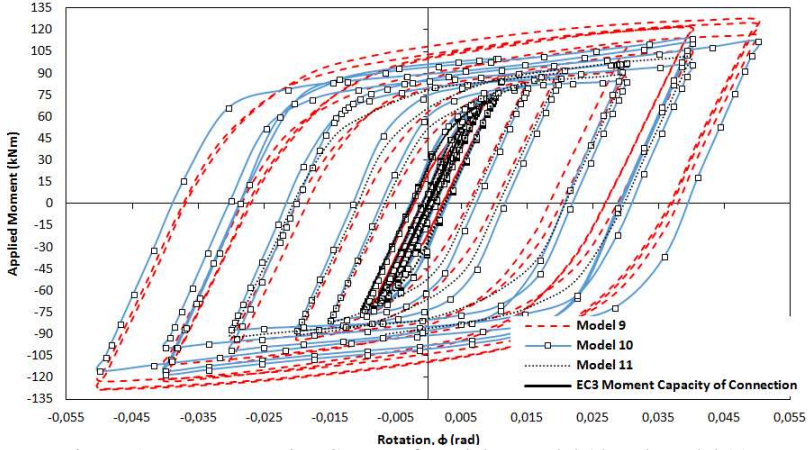
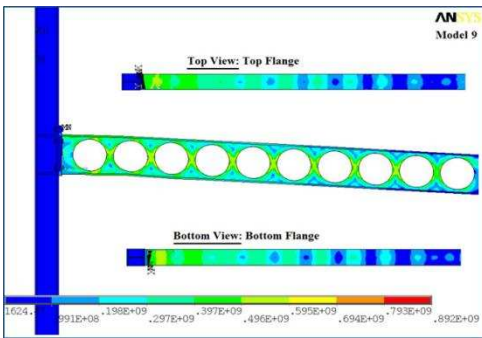
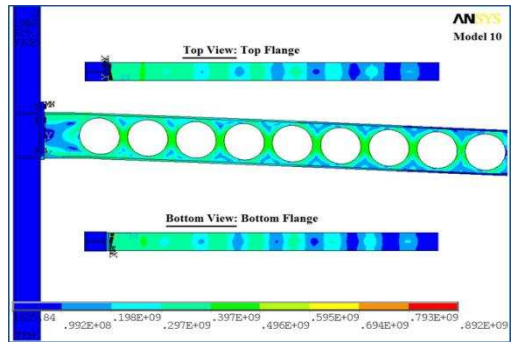


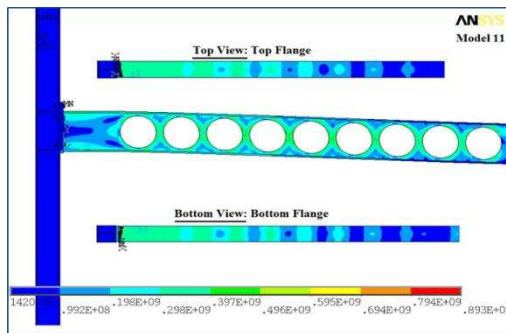
Figure 5. Moment-rotation Curves of Model 9, Model 10 and Model 11.



Model 9: loading at 155.1mm, cycle 32



Model 10: loading at 155.1mm, cycle 31



Model 11: loading at 62.1mm, cycle 36

Figure 6. Von-Mises stress contour plots of Set 2.

Model 9 achieved the full 64 load steps corresponding to the 32 cycles. It reached an ultimate rotational capacity of 0.05radian and the higher maximum moment of 128.51kNm. The stress is transferred into the beam creating a Vierendeel mechanism, while the formation of plastic hinges in the vicinity of circular openings is visible. The column, including its shear panel zone as well as the end-plate, experienced low intensity stresses, while the stress in the bolts decreased significantly to a maximum of about 850MPa. Additionally, having closely spaced web openings resulted in a balanced distribution of the transferred stresses over the adjacent web openings. The critical stresses of 565MPa were located along the length of the beam, away from the joint region. However, some high stresses remained in the vicinity of the welds. The distance $S=200\text{mm}$ is deemed to be too narrow to mobilise the stresses away enough from the face of the column.

Model 10 failed to converge at load step 61 corresponding to cycle 31. The ultimate rotational capacity of 0.05radian is however achieved. Observing the stress distribution, changes obtained in Model 10 resulted in a similar but improved behaviour in comparison to Model 9. The desired weak beam-strong column mechanism is achieved, while lateral torsional buckling is recorded in higher maximum moment. The column, including its web panel zone as well as the end-plate, experiences little to no stress; the stress in the bolts decreases significantly to a maximum of about 850MPa. The critical stresses of 560MPa are located along the length of the beam and not in the critical area where the beam is connected to the column, with only some stress in the vicinity of the welds, as compared to Model 9. The dimension of $S=350\text{mm}$ is deemed to be ideal to move the critical zone away from the face of the column and achieve enhanced structural performance.

Model 11 failed to converge at load step 52 corresponding to cycle 26. It achieved an ultimate rotational capacity of only 0.04radian. Observing the stress distribution, it is concluded that the changes made in Model 11 resulted in a very similar behaviour to Model 10. The shear panel zone and the column experiences low stress while the stress in the bolts decreases significantly to a maximum of about 850MPa. The critical zone (of approximately 500MPa) is found somewhere along the length beam far from the joint, with very low stress in the vicinity of the welds. The dimension of $S=500\text{mm}$ is deemed to be capable to mobilise the critical stresses away from the face of the column but an ultimate rotational capacity of 0.04radian compared to 0.05radian for $S=350\text{mm}$ is now obtained.

4 CONCLUDING REMARKS, SUGGESTIONS AND LIMITATIONS

This study presents a finite element computational step-by-step work introducing partially restrained extended end-plate beam-to-column connections with single and multiple large circular web perforations along the beam subjected to cyclic quasi-static loading. It is essential for the connection to move the stresses to the desired location creating a weak beam-strong column mechanism acting as a ductile seismic fuse through the formation of plastic hinges.

The study indicates that such connections behave in a satisfactory manner and provide an enhanced performance in terms of stress distribution when subjected to cyclic loading, especially when the web openings are located at a particular distance from the face of the column. The desirable weak beam-strong column mechanism was accomplished by the introduction of web openings, proving the performance of RWS connections to be used in seismic resistant designs.

Models with uniform material properties were also examined (S355 for all components except of the bolts with Class 10.9), as the initial difference in material properties taken from the specific experiment hindered the desired mechanism. The addition of column stiffeners, similar to practice, was investigated as the flanges restrain the out-of-plane buckling. Specimens with closely spaced web openings demonstrated positive results, with the latter ones mobilising the critical stresses in the vicinity of the first web opening.

Column face distance, S , of 520mm decreases the ultimate rotational capacity from 0.05radian to 0.04radian, while distance of 200mm or less leads to critical stress concentration very close to the columns' face and the connections' components. The ideal distance, S , was therefore identified as being 350mm (i.e. $1.2d_o$ or $0.96h$).

Limitations of this study suggest future work to be conducted regarding the use of perforated beams in the aseismic design of steel MRFs. This study is part of an extensive research project investigating different types of connections and the use of novel patented elliptically-based web openings, aiming to establish comparisons of seismic and progressive collapse codes and design guidelines.

REFERENCES

- [1] Eurocode 3 [2005]: Design of Steel Structures – Part 1: General Rules and Rules for Buildings, EN 1993-1-1, Brussels, Belgium.
- [2] EC8. Part 3: Design of Structures for Earthquake Resistance. Assessment and Retrofitting of Buildings. EN 1998-3, June 2005.
- [3] Popov, E.P., Yang, T.-S., and Chang, S.-P. 1998. Design of Steel MRF Connections Before and After 1994 Northridge Earthquake. *Engineering Structures*, vol. 20, pp. 1030-1038.
- [4] Lee, C., and Kim, J. 2007. Seismic Design of Reduced Beam Section Steel Moment Connections with Bolted Web Attachment. *Journal of Constructional Steel Research*, vol. 63, pp. 522-531.
- [5] Pachoumis, D., Galoussis, E., Kalfas, C., and Christitsas, A. 2009. Reduced Beam Section Moment Connections Subjected to Cyclic Loading: Experimental Analysis and FEM Simulation. *Engineering Structures*, vol. 31, pp. 216-223.
- [6] Tsavdaridis, K.D., Faghih, F., and Nikitas, N. 2014. Assessment of Perforated Steel Beam-to-Column Connections Subjected to Cyclic Loading. *Journal of Earthquake Engineering*, vol.18, issue 8, pp. 1302-1325.
- [7] Tsavdaridis, K.D., and D'Mello, C. 2011. Web Buckling Study of the Behaviour and Strength of Perforated Steel Beams with Different Novel Web Opening Shapes. *Journal of Constructional Steel Research*, vol. 67, pp. 1605-1620.
- [8] Tsavdaridis, K.D., and D'Mello, C. 2012. Optimisation of Novel Elliptically-Based Web Opening Shapes of Perforated Steel Beams. *Journal of Constructional Steel Research*, vol. 76, pp. 39-53.
- [9] Tsavdaridis, K.D., and Pilbin, C., 2014. Assessment of a Pre-Northridge Steel Connection with Novel Beams under Progressive Collapse. *Journal of Constructional Steel Research*. (accepted, in press)
- [10] FEMA 350, "Recommended seismic design criteria for the new steel moment frame Buildings", Report no. FEMA 350, SAC Joint Venture, CA, 2000.
- [11] Yang, Q., Li, B., and Yang, N. 2009. Aseismic Behaviors of Steel Moment Resisting Frames with Opening in Beam Web. *Journal of Constructional Steel Research*, vol. 65, pp. 1323-1336.
- [12] Díaz, C., Victoria, M., Marti, P., and Querin, O. 2011. FE Model of Beam-to-Column Extended End-Plate Joints. *Journal of Constructional Steel Research*. vol. 67, pp. 1578-1590.
- [13] Tsavdaridis, K.D., and D'Mello, C. 2012. Vierendeel Bending Study of Perforated Steel Beams with Various Novel Web Opening Shapes through Nonlinear Finite-Element Analyses. *Journal of Structural Engineering (United States)*, vol. 138, pp. 1214-1230.